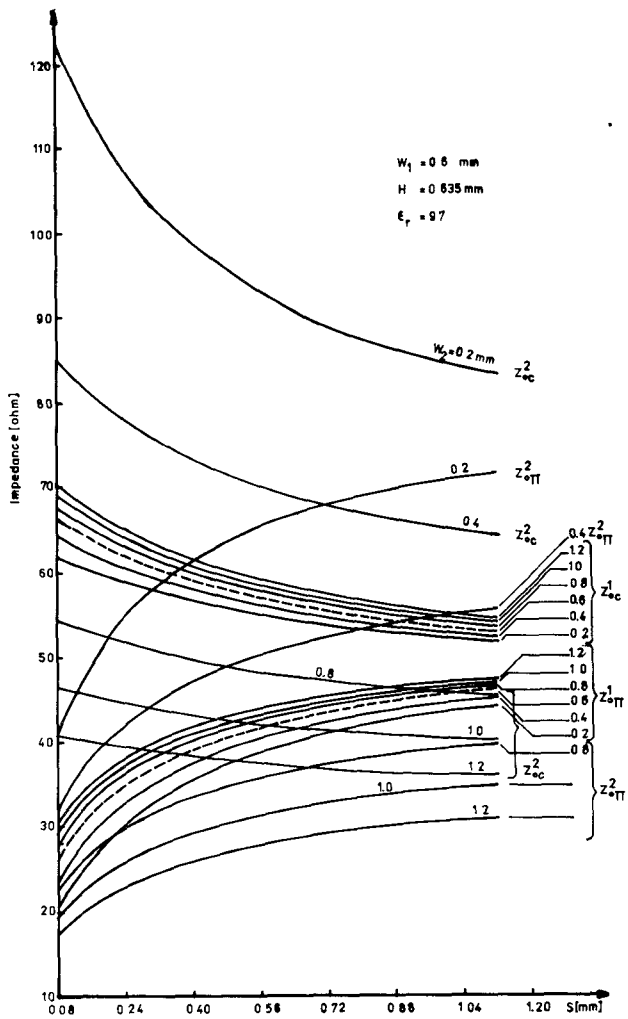

Fig. 7. Variation of mode impedances of asymmetric coupled microstriplines with their separation.

lines are also higher than those of Judd *et al.* given in Table I, and are on the side of the higher results given in this table.

In order to allow the design of various microstrip structures using asymmetric coupled lines (such as filters, couplers, etc.), a set of design curves for different geometric configurations were calculated and are shown in Fig. 7. These curves were calculated for the quasi-static case, and the effect of dispersion can be accounted for by using the introduced dispersion model. In this set of curves, the width of the first line W_1 was taken 0.6 mm since it represents approximately a 50-Ω line on alumina substrate ($\epsilon_r = 9.7$, $H = 0.635$ mm). The width of the second line W_2 was allowed to vary from 0.2 mm up to 1.2 mm in steps of 0.2 mm. The symmetric case where $W_1 = W_2 = 0.6$ mm is shown by the dotted line curves.

VI. Conclusion

A network analog method was chosen to calculate the mode numbers, the effective dielectric constants, and the mode impedances of two asymmetric coupled microstrip-lines. This method has the advantage of reducing the computation time as compared with the ordinary finite difference method. A dispersion model was introduced which can be considered as an extension of Getsinger's dispersion model for two symmetric coupled lines. The obtained numerical results taking into consideration the dispersion effect were found to be in a good agreement with the only available published data. A set of design curves for different geometric dimensions of the two lines was presented which should prove to be useful in the design of various microstrip structures.

References

[1] R. H. Jansen, "Fast accurate hybrid mode computation of nonsymmetrical coupled microstrip characteristics," in *Proc. 7th Eur. Microwave Conf.*, (Copenhagen), 1977, pp. 135–139.
[2] J. L. Allen, "Non-symmetrical coupled lines in an inhomogeneous dielectric medium," *Int. J. Electronics*, vol. 38, pp. 337–347, 1975.
[3] V. K Tripathi, "Asymmetric coupled transmission lines in an inhomogeneous medium," *IEEE Trans. Microwave Theory Tech.*, vol. MTT-23, pp. 734–739, Sept. 1975.
[4] V. K. Tripathi, "Equivalent circuits and characteristics of inhomogeneous nonsymmetrical coupled-line two-port circuits," *IEEE Trans. Microwave Theory Tech.*, vol. MTT-25, pp. 140–142, Feb. 1977.
[5] R. A. Speciale, "Even- and odd-mode waves for non-symmetrical coupled lines in nonhomogeneous media," *IEEE Trans. Microwave Theory Tech.*, vol. MTT-23, pp. 897–908, Nov. 1975.
[6] R. E. Collin, *Field Theory of Guided Waves*. New York: McGraw-Hill, 1960, ch. 4.
[7] R. Garg and I. J. Bahl, "Characteristics of coupled microstriplines," *IEEE Trans. Microwave Theory Tech.*, vol. MTT-27, pp. 700–705, July 1979.
[8] B. L. Lennartsson, "A network analogue method for computing the TEM characteristics of planar transmission lines," *IEEE Trans. Microwave Theory Tech.*, vol. MTT-20, pp. 586–591, Sept. 1972.
[9] W. J. Getsinger, "Dispersion of parallel-coupled microstrip," *IEEE Trans. Microwave Theory Tech.*, vol. MTT-21, pp. 144–145, Mar. 1973.
[10] W. J. Getsinger, "Microstrip dispersion model," *IEEE Trans. Microwave Theory Tech.*, vol. MTT-21, pp. 34–39, Jan. 1973.
[11] T. G. Bryant and J. A Weiss, "Parameters of microstrip transmission lines and of coupled pairs of microstrip lines," *IEEE Trans. Microwave Theory Tech.*, vol. MTT-16, pp. 1021–1027, Dec. 1968.
[12] S. V. Judd *et al.*, "An analytical method for calculating microstrip transmission line parameters," *IEEE Trans. Microwave Theory Tech.*, vol. MTT-18, pp. 78–87, Feb. 1970.
[13] S. Akhtarzada *et al.*, "The design of coupled microstrip lines," *IEEE Trans. Microwave Theory Tech.*, vol. MTT-23, pp. 486–492, June 1972.
[14] R. P. Coats, "An octave-band switch-line microstrip 3-b diode phase shifter," *IEEE Trans. Microwave Theory Tech.*, vol. MTT-21, pp. 444–449, July 1973.
[15] R. H. Jansen, "High-speed computation of single and coupled microstrip parameters including dispersion, high-order modes, loss and finite strip thickness," *IEEE Trans. Microwave Theory Tech.*, vol. MTT-26, pp. 75–82, Feb. 1978.

Microwave Characteristics of an Optically Controlled GaAs MESFET

HIDEKI MIZUNO

Abstract —**This paper presents the results of an experimental investigation of microwave characteristics of a GaAs MESFET under optically direct-controlled conditions. The gain, drain current, and *S*-parameters were measured under various optical conditions in the frequency region from 3.0 GHz to 8.0 GHz, and it was found that they can be controlled by**

Manuscript received December 19, 1982; revised March 9, 1983.
The author is with Yokosuka Electrical Communication Laboratory, NTT, 1-2356, Take, Yokosuka-shi, Kanagawa-ken, 238-03 Japan. Telephone (0468) 59-3266

0018-9480/83/0700-0596$01.00 ©1983 IEEE

varying the incident light intensity in the same manner as when varying the gate bias voltage. As applications of this phenomenon, optical/microwave transformers and an optically switched amplifier were investigated.

I. Introduction

In recent years, considerable attention has been given to optically controlled GaAs MESFET's [1]–[4]. By utilizing light to control the microwave characteristics of a GaAs MESFET, many charming applications involving optically controlled GaAs MESFET's become feasible. Examples are optically controlled amplifiers and optically controlled oscillators. These amplifiers and oscillators will be used as an optical/electrical transformer which directly converts optical signals into microwave signals. In the past, the characteristics of the GaAs MESFET have been examined under the condition where the GaAs MESFET functions as a dc detector of light [2]–[4]. However, the microwave characteristics of the GaAs MESFET under optically direct-controlled conditions have not yet been clarified.

This paper describes an experimental investigation of the microwave characteristics of an optically direct-controlled GaAs MESFET, and presents the results of a feasibility study for such applications as optical/microwave transformers.

II. Experiments

A. GaAs MESFET and Light Source

The GaAs MESFET used in the study is an 0.5-μm gate-length device (NE388, NEC) in a stripline type ceramic package with the top lid removed. The doping level and the thickness of the active layer are 2.5×10^{17} cm^{-3} and 0.15 μm, respectively [5]. The GaAs MESFET is fixed on a transistor test fixture (HP-11608A), as shown in Fig. 1. Light is incident on the GaAs MESFET with an optical fiber. The distance between the fiber end and the GaAs MESFET is about 1 mm.

The light source is a fiber-coupled semiconductor laser, with a wavelength of 0.829 μm, and the maximum output power is about 2 mW. The output power is varied by an optical attenuator, and measured by an optical power meter. The laser can be modulated over the frequency region from 10 kHz to 300 MHz. A YAG laser was also used to investigate the wavelength dependent characteristics.

B. Gain–Drain Current Versus Light Intensity

The gain (input versus output microwave power ratio) and drain current (I_{ds}) were measured while varying the gate-source voltage (V_{gs}) or incident light intensity. The microwave input power was set to be about -10 dBm in order to obtain a linear function. Fig. 2 shows the results.

In Fig. 2(a), gain and I_{ds} are varied as a function of V_{gs} with the GaAs MESFET not exposed to light. At the maximum gain (point A), the GaAs MESFET functions as an amplifier with a gain of 7.5 dB. The bias conditions are: $V_{gs}=-2.7$ V, $I_{ds}=13.6$ mA. At point B, where the GaAs MESFET is biased so as to be pinched off, the bias conditions are $V_{gs}=-3.6$ V and $I_{ds}=0.2$ mA.

Fig. 2(b) shows gain and I_{ds} versus incident light intensity when the GaAs MESFET is biased so as to be pinched off ($V_{gs}=-3.6$ V). The gain and I_{ds} increase with increasing incident light intensity. At point C, where I_{ds} is equal to the value at point A (13.6 mA), the incident light intensity is 0.14 mW.

Fig. 3 summarizes gain versus frequency with varying I_{ds}. In Fig. 3, a solid line shows the gain when I_{ds} is controlled by V_{gs}. A broken line shows the gain when I_{ds} is controlled by the incident light intensity, with a constant dc bias. Each set of a solid and a broken line shows the gain when the GaAs MESFET has the same I_{ds} denoted at the left of the lines. The incident light power exposed for control of I_{ds} is similarly shown at the right of the lines.

From these experiments, it is found that the gain and I_{ds} of a GaAs MESFET can be controlled by the incident light intensity in the same manner as when varying the V_{gs}.

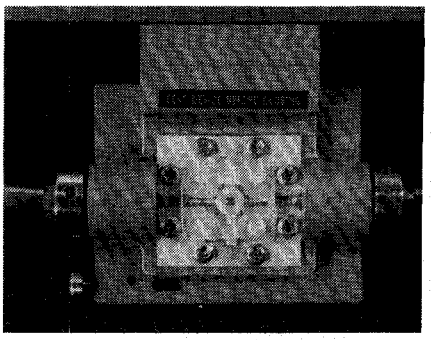

Fig. 1. GaAs MESFET installed in transistor test fixture.

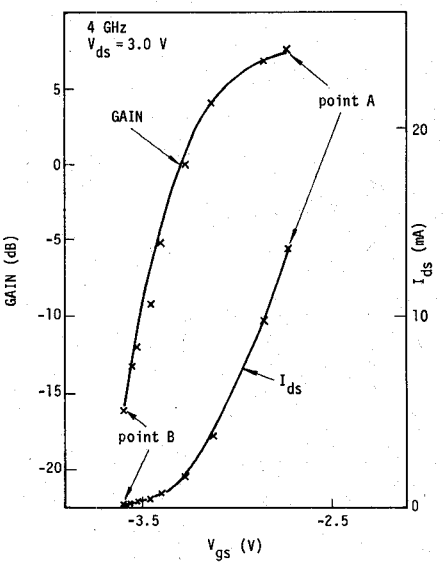

(a)

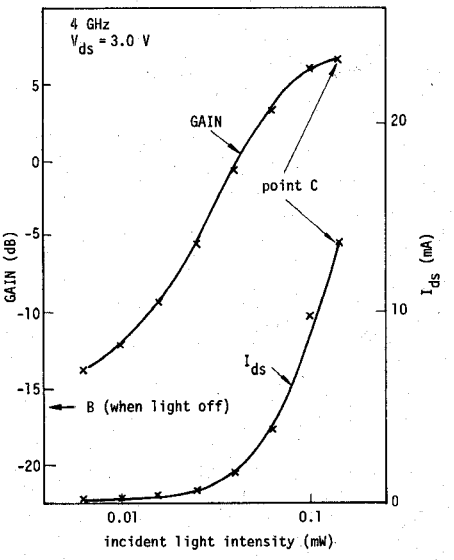

(b)

Fig. 2. Gain and drain current I_{ds}. (a) Gain and drain current versus gate bias voltage V_{gs}. (b) Gain and drain current versus incident light intensity.

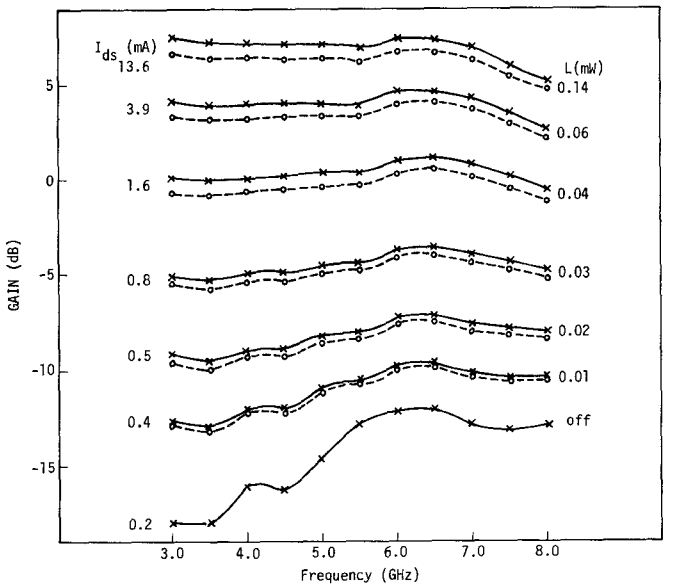

Fig. 3. Gain versus frequency with the same drain current. (Solid line shows gain controlled by V_{gs}; broken line shows gain controlled optically.)

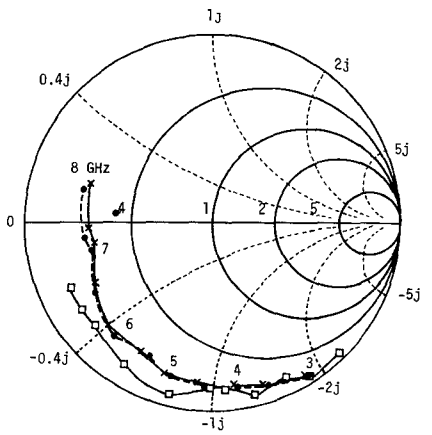

Fig. 4. S_{11} of optically/electrically controlled GaAs MESFET.

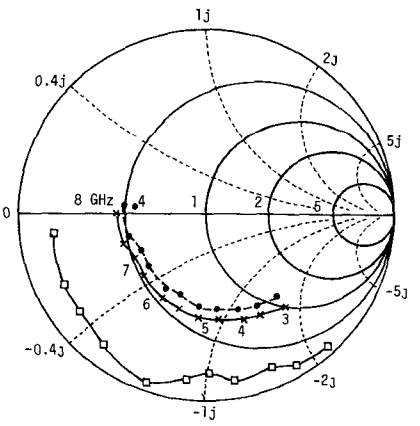

Fig. 5. S_{22} of optically/electrically controlled GaAs MESFET.

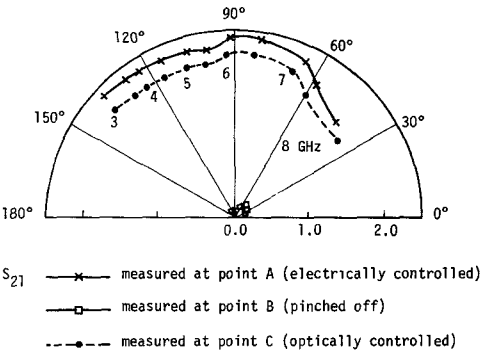

Fig. 6 S_{21} of optically/electrically controlled GaAs MESFET.

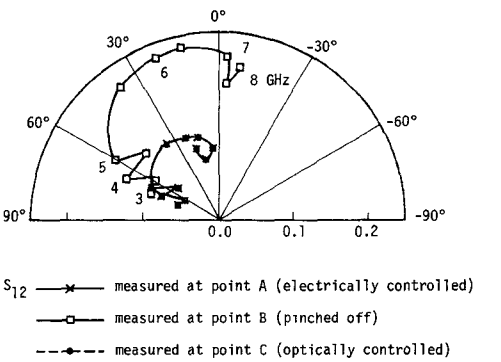

Fig. 7. S_{12} of optically/electrically controlled GaAs MESFET.

C. Measurement of S-Parameters

S-parameter measurements are carried out in the frequency region from 3.0 GHz to 8.0 GHz for bias conditions as shown at points A, B, and C in Fig. 2. Figs. 4 and 5 show the input and output reflection coefficients S_{11} and S_{22}, respectively. At points A and C, S_{11} and S_{22} show the same characteristics.

Fig. 6 shows the transverse gain S_{21}. At points A and C, S_{21} is greater than unity and the GaAs MESFET functions as a small signal amplifier.

Fig. 7 shows the reverse gain S_{12}. S_{12} at point C shows the same characteristics as at point A in the frequency region from 3.0 GHz to 8.0 GHz.

Although S-parameters at points A, B, and C are shown in Figs. 4–7, S-parameters at intermediate drain current levels change continuously from values at point A or C to those at point B. S-parameters of the optically controlled GaAs MESFET are shown to behave in the same manner as the electrically controlled one. This fact suggests that an optically controlled GaAs MESFET circuit can be designed in a similar manner to an electrically controlled circuit if I_{ds} is the same for both designs.

III. Applications of the Optically Controlled GaAs MESFET

As a result of carrying out S-parameter measurements, it was found that the incident light changes the gain and drain current in the same manner as when the gate bias voltage is varied. Therefore, the optically controlled GaAs MESFET can be regarded as a dual-gate FET: the first gate is electrical and the second gate is optical. The feasibility of such devices as optical/microwave transformers and an optically switched amplifier is examined.

A. Optical/Microwave Transformer

Fig. 8 shows schematic diagrams for two optical/microwave transformers. Fig. 8(a) shows a transformer consisting of an

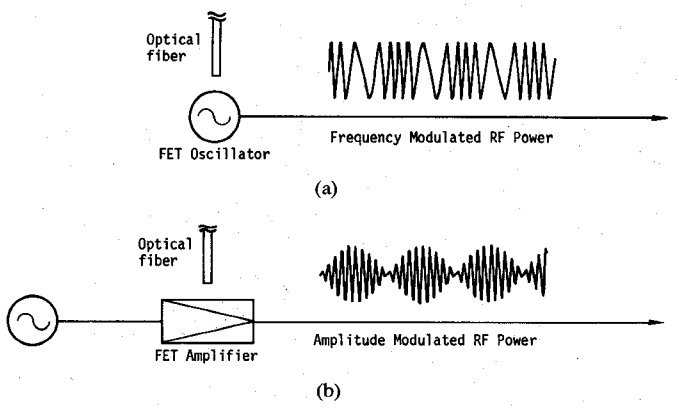

Fig. 8. Schematics for optical/microwave transformers. (a) Optical/FM microwave signals. (b) Optical/AM microwave signals.

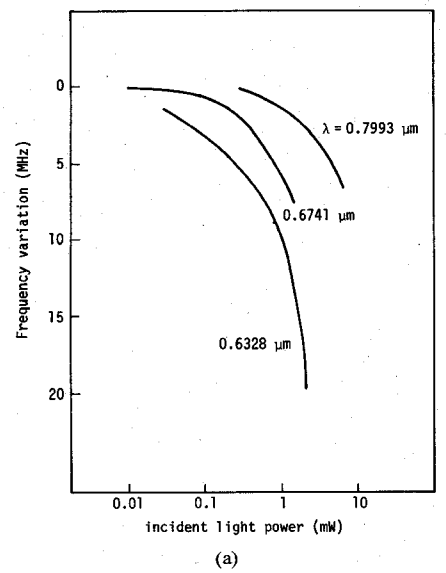

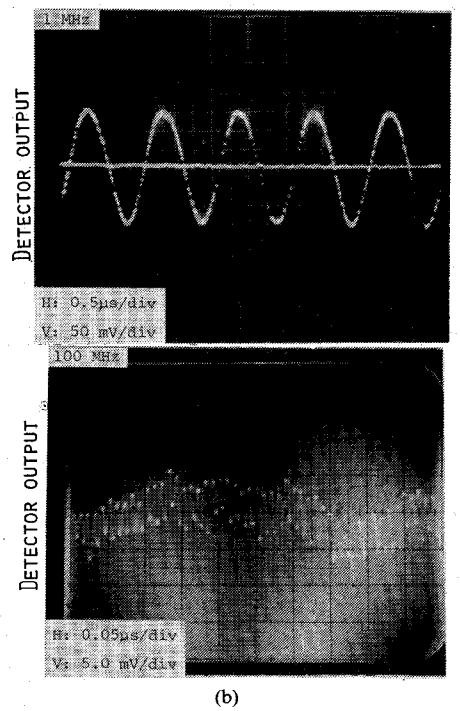

Fig. 9. Microwave characteristics of optical/microwave transformers. (a) Frequency variation of GaAs MESFET oscillator. (b) Output signals of GaAs MESFET amplifier. Incident light intensity modulated at 1 MHz and 100 MHz.

optically controlled oscillator. This transformer converts optical signals into frequency modulated microwave signals. Fig. 8(b) also shows a transformer converting optical signals into amplitude modulated microwave signals. These two types of optical/microwave transformers were fabricated in order to examine electrical characteristics.

Fig. 9(a) shows the frequency variation of the GaAs MESFET oscillator when the incident light intensity was varied. The free-running oscillation frequency is 21.4 GHz. The GaAs MESFET is mounted in a waveguide housing [6]. In Fig. 9(a), the wavelength of the light is also varied. When the wavelength of the light decreases, the frequency variation increases. It can thus be seen that the GaAs MESFET is sensitive to the frequency of the incident light. This kind of oscillator can be used as an optical/FM microwave transformer.

Fig. 9(b) shows the microwave output power of the GaAs MESFET amplifier detected by a crystal detector when the incident light amplitude is modulated at 1 MHz and 100 MHz. As shown in Fig. 9(b), the microwave output power has been modulated at 1 MHz and 100 MHz. The GaAs MESFET has a response speed of 10 ns at 100 MHz. This kind of amplifier can be used as an optical/AM microwave transformer.

B. Optically Switched FET Amplifier

Another application of the optically controlled GaAs MESFET is as an optically switched amplifier. In the 'on' condition, the GaAs MESFET is exposed to incident light with a power of 0.14 mW. Gain characteristics have been presented in Fig. 3. The amplifier works only when the GaAs MESFET is exposed to the light. In the 'off' condition, the light is turned off. Isolation between the 'on' condition and 'off' conditions is more than 22 dB at 4 GHz as shown in Fig. 3. Furthermore, the switched amplifier is of the normally-off type, and the ratio of the power consumption at 'on' and 'off' conditions is 40.8 mW to 0.7 mW (1.7 percent). This kind of amplifier can be used as an SPST switch, and is suitable for use as a large-scale switch because interference between microwave signals and control-line signals is very small.

IV. Conclusion

The fundamental microwave characteristics of the optically direct-controlled GaAs MESFET were examined. It was found that incident light intensity changes the gain, drain current and *S*-parameters in the same manner as when the gate bias voltage is varied. In other words, the GaAs MESFET works as a dual-gate FET: the incident light is equivalent to the second gate. Further, the optical/microwave transformer and optically switched amplifier were examined. The results obtained in this paper show the feasibility of using optically direct-controlled GaAs MESFET for high-speed and high-sensitivity applications.

Acknowledgment

The author wishes to thank Drs. H. Tohyama, H. Odate, I. Kobayashi, T. Sugeta, and M. Akaike of the Electrical Communication Laboratory, NTT, for their encouragement and valuable discussions.

References

[1] F. J. Moncrief, "LED's replace varactors for tuning GaAs FETs," *Microwaves*, pp. 12–13, Jan. 1979.
[2] J. C. Gammel and J. M. Ballantyne, "The OPFET: A new high speed optical detector," in *IEEE Int. Electron Devices Meet. Dig.*, Dec. 1978, pp. 120–123.
[3] C. Baack *et al.*, "GaAs MESFET: A high-speed optical detector," *Electron. Lett.*, vol. 13, no. 7, pp. 193, Mar. 1977.
[4] T. Sugeta and Y. Mizushima, "High speed photoresponse mechanism of GaAs-MESFET," *Japan. J. Appl. Phys.*, vol. 19, no. 1, Jan. 1980.

[5] M. Ogawa, K. Ohata, T. Furutsuka, and N. Kawamura, "Submicron single-gate and dual-gate GaAs MESFET's with improved low noise and high gain performance," *IEEE Trans. Microwave Theory Tech.*, vol. MTT-24, pp. 300–305, June 1976.
[6] H. Mizuno, "GaAs FET mount structure design for 30-GHz-band low noise amplifiers," *IEEE Trans. Microwave Theory Tech.*, vol MTT-30, pp. 854–858, June 1982.

Measured Temperature-Dependence of Attenuation Constant and Phase Velocity of a Superconducting PbAu/SiO/Pb Microstripline at 10 GHz and 30 GHz

RALF PÖPEL

Abstract—**Measured results for the temperature dependence of the attenuation constant and phase velocity of a superconducting microstripline at 10 GHz and 30 GHz are presented here for the first time. At 9.1 GHz the attenuation constant of a PbAu/SiO/Pb microstripline with a dielectric height of 880 nm decreases from 1.6 dB/m to 0.04 dB/m going from 4.2 K to 2.0 K, while at 27.3 GHz a decrease from 2.6 dB/m to 0.09 dB/m going from 3.0 K to 1.7 K was measured.**

The calculated and measured temperature dependence of the phase velocity are in good agreement. The measured values for the attenuation constant together with the estimate of conductor losses from the Mattis–Bardeen theory, taking radiation losses and surface roughness into account, lead to an upper limit estimate for the loss factors of SiO.

I. Introduction

In contrast to waveguide technology, with the aid of stripline technology, circuits requiring a much smaller space and weighing considerably less can be constructed. Stripline circuits also have a lower heat conductivity and heat capacity. This is particularly advantageous for cryogenic microwave circuits. Moreover, cryogenic circuits with many planar and small Josephson elements can be placed on one substrate. Complex circuits can be built up in this way, e.g., logic circuits of Josephson computer technology [1], circuits with many dc series-connected Josephson elements for voltage standards [2], or Josephson arrays for microwave devices [3].

For low-temperature operation, stripline cross sections can be made considerably smaller than for use at room temperature [4]. Although with decreasing dielectric heights h the conductor losses for microstriplines increase considerably, the use of superconducting material for groundplane and strip can keep these losses down.

An advantage is that radiation losses which are important at frequencies $\gtrsim 10$ GHz for dielectric heights of the order of 0.5 mm decrease strongly with smaller dielectric heights.

For microstriplines with strip width $w \gg h$ the parallel plate line equation is valid in good approximation

$$Z_L = \frac{\eta}{\sqrt{\epsilon_r}} \cdot \frac{h}{w} \tag{1}$$

with $\eta = 120\ \pi\Omega$ – wave impedance in free space, ϵ_r is the dielectric constant, h is the dielectric height, and w is the strip width.

From (1) we see that to obtain a definite wave impedance Z_L (e.g., for matching purposes), with smaller dielectric heights the strip width must also become smaller. Indeed, two strips can be placed closer together without any considerable coupling between them. These two effects allow a higher packing density to be achieved. Superconducting microstriplines of this kind have been examined both theoretically [5] and experimentally.

Kautz [6] has measured the attenuation constant α_0 of $Nb/Nb_2O_5/PbAu$ microstriplines below 500 MHz and found a frequency independent Nb_2O_5 loss factor of about $2 \cdot 10^{-3}$ at 4 K. The temperature dependence of phase velocity has also been measured by Mason and Gould [7] on Ta/Ta-oxide/In microstriplines below 500 MHz. Because the superconducting microstriplines are for use at microwave frequencies or for picosecond pulse transmission, 10-GHz attenuation measurements of $Nb/Nb_2O_5/PbInAu$ lines were performed at 4.2 K [8]. The dielectric loss factor of Nb_2O_5 at 4.2 K was confirmed to be rather high, i.e., $\tan\delta \approx 2.1 \cdot 10^{-3}$. Because of an expected lower $\tan\delta$ of SiO and because the use of SiO is widespread in circuits with Josephson junctions [1], lines with SiO dielectric were examined. Measuring results are presented here for the temperature dependence of the attenuation constant α_0 and phase velocity v_φ for a superconducting PbAu/SiO/Pb microstripline with a dielectric height of $h = 880$ nm at frequencies of about 10 GHz and 30 GHz. These results are discussed in conjunction with current theories.

II. Theoretical Background

An investigation of superconductors with the help of resonant cavities is possible at microwave frequencies. The measured values of the surface resistance R_s can be approximated quite well by equations from the BCS theory if the energy gap 2Δ, or the mean free path l (of normal electrons), are used as approximation factors [9]. It is possible to measure the loss factors of dielectrics, inserted in a superconducting resonant cavity. In this way, Meyer [10] measured the loss factors of synthetic materials, such as quartz glasses and natural quartz, in the frequency range from 0.2 GHz to 7 GHz at temperatures between 2.0 K and 4.2 K. However, there are no measuring results of the surface resistance of PbAu and of the loss factor of SiO at microwave frequencies and low temperatures.

When we investigate a superconducting microstripline, according to the equation

$$\alpha_0 = A \cdot \alpha_c + \alpha_d + \alpha_r \tag{2}$$

conductor losses, dielectric losses, and radiation losses must be taken into account, where α_c, α_d, and α_r are the attenuation constants due to conductor losses, dielectric losses, and radiation losses, respectively. In addition, the factor A accounts for the influence of surface roughness.

In 1960, Swihart [5] derived formulas for calculating α_c, α_d, and the phase velocity v_φ of superconducting microstriplines with $w \gg h$. These equations are the solutions of the classical model of superconduction, namely of the two London equations, the two-fluid model, Maxwell's equations, isotropic material distribution,

Manuscript received December 29, 1982; revised March 10, 1983 This work was supported in part by the Deutsche Forschungsmeinschaft.
The author is with the Physikalisch-Technische Bundesanstalt, Bundesallee 100, West Germany.

0018-9480/83/0700-0600$01.00 ©1983 IEEE